Response to referee 3

General Comments

This manuscript addresses retrieval of surface roughness length on ice sheets using ICESat-2 data profiles. Empirically based retrieval of surface roughness length from satellite observations is an enormously important task; the parameter modulates energy fluxes between the atmosphere and the cryosphere, changes in both space and time, and is poorly known. Current methods of retrieval generalize single point measurements to large expanses of the ice sheet; not only do we not have spatially resolved estimates of this parameter, we lack comprehensive understanding of the variance, range, and uncertainty of the parameter. Thus, the present work is extremely timely and important to the community at large. That said, there are several shortcomings with this work; the applicability is limited to a narrow range of surface types and elevations that form a minority of the ice sheet area, the measurements themselves have large uncertainties and are resolved for specific wind directions that do not match prevailing katabatic patterns, and the validation strategy and data are marginally matched to the task. This study is undeniably useful as it forms a basis for future work to build on; the problem under study is a hard task, and incremental progress should be recognized and iterated with new, separate publications that extend to the rest of the ice sheet. In short, this work is worthy of publication following revisions– there are specific tasks and issues that should be addressed in the revision, and other issues that can be deferred as 'out of scope' and addressed in distinct publications rather than in the current work.
We thank the referee for his time and his comments. In the text below we respond point-by-point and discuss the changes to the work. The referee comments are written in black. Our answer to each comment is written below in blue. The proposed changes to the original manuscript are then highlighted in red.

Specific Comments

The spatial and temporal mismatch of the validation data from S5 is the largest issue with the current submission. The S5 site is the only location that ties together all three components of data used in this study– structure from motion DEMs, ICESat-2 tracks, and empirical measurements of surface roughness length by in situ measurements. Although both the 'A' and 'B' structure for motion boxes are bigger, and overlap with ICESat-2 tracks, the lack of weather station data forces S5 to be the primary validation loci, despite the smaller than desired area/fetch coverage. The large temporal gap (September DEM and in situ measurements, March ICESat-2 data) isn't ideal, and needs to be fixed

(preferably), or explained and justified in greater detail. ICESat-2 was operating in September of 2019– why isn't there coincident data provided? Looking at the track crossings, it appears that September 24 was cloudy to the point of signal loss, but this isn't explained...signal from September 12th is stronger and appears to cover and cross over S5, so why wasn't this data used? What is the justification and the trade space between small spatial mismatches vs large temporal mismatches? Why March? Having data coincident in both time and space for the validation is ideal, and a strong case with reasoning and justification needs to be made as to why September data was not used and/or was not tractable for use.
The single reason why we only use a single ICESat-2 measurement at S5 in March 2019 is because this is the only measurement that exactly overpasses the automatic weather station (AWS). This can be visualized in attached Figure R1. Before 1 April 2019, the ATLAS instrument was not pointing at the reference ground track (RGT), but $\approx$ 1.5 km off, over the K-transect. Conveniently this brief mismatch meant that the ICESat-2 data (track 1169, cycle 02, segment 05, beam GT1L) exactly overpassed the AWS S5 in March 2019 within a few meters, taking into account ice velocity ($\approx$ 100 m yr^{-1}). After 1 April 2019, ICESat-2 was nominally pointing at the RGT again. Unfortunately the closest ground track number 1169 is located 1.5 km West of S5, which prevents a direct comparison between ICESat-2 track 1169 and AWS S5. Yet track 1344 (beam GT1R & GT1L, segment 03) overpassed S5 during on 25 June and 24 Sep 2019, but the signal cannot be retrieved due to clouds. A possibility to have more coincident data would be to move the location of the AWS. However the practical limitations greatly outweigh the scientific added value, due to the crevassed surroundings which considerably limits the amount of areas suited for safe instrument deployment. Besides, we would still not be able to directly compare AWS data to ICESat-2 tracks because of the different wind fetch directions.
We propose to add this important piece of information in the revised manuscript.

L184:
A typical geolocated photon measurement ATL03 (Neumann et al., 2019) can be seen in Fig. 3 for site S5, and in Fig. 4a for area A. Details about which ICESat-2 measurements are compared against the UAV surveys are provided in Table 2. Not more than one ICESat-2 measurement exactly overlaps each UAV survey. This is mainly due to the presence of clouds and due to changes in laser pointing orientations in other ICESat-2 measurements, but also due to changes in the studied locations due to ice flow.

While having structure for motion, in situ, and ICESat-2 data all be coincident is ideal, the second best approach is paired validation: coincident UAV and in situ data to validate the method, followed by coincident ICESat-2 and in situ data to validate the scaling to the 1D profile. This is especially appealing since the current work already has separate pairing that is discussed with ICESat-2 and UAV data in boxes A and B in addition to pairing of UAV and

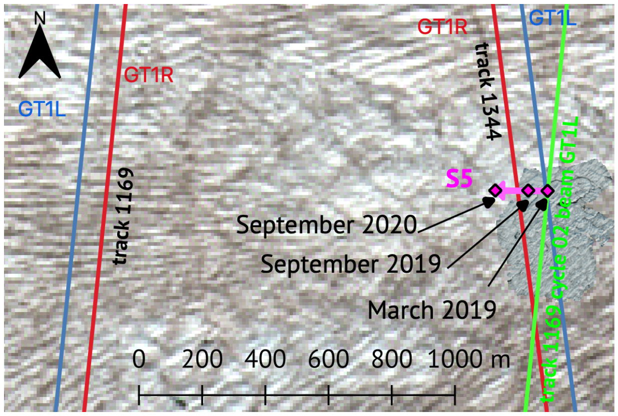

Figure R1: ICESat-2 track location with respect to AWS site S5

.

in situ data at S5; the only pairing not present is between ICESat-2 and in situ tower measurements. Even if data doesn't simultaneously overlap for all three data sets, finding an overlap between ICESat-2 and the S5 station provides the needed coverage for a compelling validation strategy. I'm unclear on if this is possible, or perhaps why it isn't possible since my expertise is more with ICESat-2 than with tower measurements. My impression is that the most of the weather stations such as S5 collect data in dense time series that are continuous save for maintenance or power outages. Is there a reason why there's not coincidence between S5 and ICESat-2, such as lack of co-occurrence that matches the prevailing wind direction? Some of this is addressed explicitly around line 320, but I'm still skeptical; if wind measurements are occurring in dense (i.e., multi-hertz) time series, brief changes from the prevailing wind direction should still occur, even if they are not sustained on the time scale of hours or days.
We thank the reviewer for pointing out two distinct issues: (1) the availability of AWS measurements during ICESat-2 overpasses, (2) the absences of wind directions in the available AWS data that match the ICESat-2 ground tracks.
Regarding issue (1), we do have year-round flux measurements using the vertical-propeller eddy covariance method (VPEC), that we compare to both the UAV and ICESat-2 modelled z_{0m} in Figure 8. We have chosen to only use data from 2017 as this has been previously published and discussed in great detail by van Tiggelen et al (*A Vertical Propeller Eddy-Covariance Method and Its Application to Long-term Monitoring of Surface Turbulent Fluxes on the Greenland Ice Sheet*. Boundary-Layer Meteorol 176, 441–463 (2020). https://doi.org/10.1007/s10546-020-00536-7). We assume that z_{0m} estimated in March-April 2017 is the same as during March 2019, and thus conclude that the modelled z_{0m} by ICESat-2 qualitatively agrees with the measurements. The quantitative analysis is not possible because of issue (2).
Regarding issue (2), the reviewer is right: brief changes in wind direction do

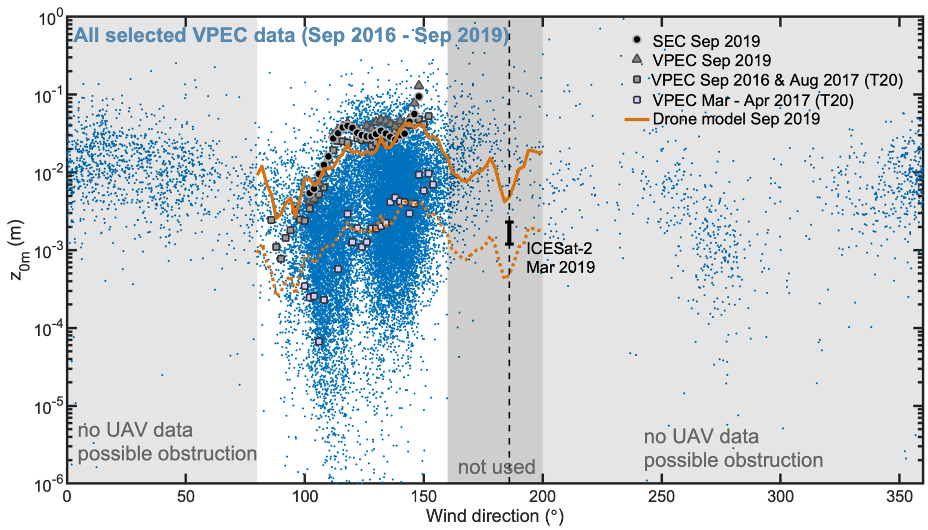

Figure R2: As in Figure 8 but including all selected VPEC measurements in the period Sep 2016 - Sep 2019

occur. Nevertheless, to estimate z_{0m} we compute the momentum flux as the covariance of the horizontal and vertical wind velocity in 30 min intervals. This down-sampling operation (from 1 measurement per 0.1 s to 1 per 30 min) removes many but not all wind directions outside the [80;160] range. Furthermore, we then only select flux measurements that pass some quality filters detailed in Van Tiggelen et al (2020), such as minimum wind speed of 3 m s^{-1}, neutral conditions, removal of non-physical values and obstructed wind direction by other structures. This leaves just a few z_{0m} estimates from AWS data for wind directions outside the [80;160] range, over the 3 years of data (Sep 2016 - Sep 2019). Especially the wind obstruction quality filter is important as it removes all measurements outside the [80;200] range. Given the large uncertainty in the estimated z_{0m} from measured fluxes, we finally average z_{0m} in bins per wind direction, and discard the few remaining points in the [160;200] wind direction range. This can be visualized in the attached Figure R2, which is the same figure as Fig 8 but showing the selected raw data (not considering the flow obstruction filter).

L143:

Vertical propeller eddy covariance (VPEC, see also T20) measurements are available at sites S5 (67.094° N, 50.069° W, 560 m) and S6 (67.079° N, 49.407° W, 1010 m) since 2016, while AWS observations are available since 1993 and 1995 for each site (Smeets et al, 2018). For this study we use eddy-covariance measurements acquired during September 2019 at site S5 and also site SHR (67.097° N, 49.957° W, 710 m), and during from September 2018 to August 2019 at site S6. All these sites are situated in the lower ablation area of the K-transect, (...).

L159:
Details about the processing steps and further data selection strategies can be found in T20. The data selection strategy removes all data points with wind directions outside the [80°;200°] interval.

Given how hydrologically active the area is, I was surprised by the lack of discussion or mention of water such as lakes and the impact on the retrieval process. Figure 3 shows a profile that appears to have multiple surfaces between 100 and 150 meters that may be water ponding. Around line 195 or 200 would be an appropriate place to discuss this, given the discarding of photons below the median which will help with water surfaces.
We thank the reviewer for this interesting application. We propose to mention this in the updated manuscript. However deriving surface water heights from multiple reflections is outside the scope of this study. Interestingly, the dip in Figure 3 between 100 m and 150 m is a narrow meltwater channel ($\approx$ 1m in width) located in a elevation depression of $\approx$ 30 m in width (see also Figure 2c). Therefore we do not believe this dip is caused by multiple reflections, but that it causes a cluttering of photons due to the locally steep topography.

L201:
We set the window length to 50 m. The previous selection strategy could also be applied for retrieving the surface in the case of multiple reflections (e.g. shallow supraglacial lakes), but this was not tested.

The algorithm only uses a single profile; probably fine for this paper, but difficulties in determining the width parameter (or whether a given obstacle meets the width threshold) can likely be improved by examining both of the pairs to assess obstacle persistence in the across track. Similarly, I expect that cross track estimation of surface roughness is feasible at track cross over points given the double beam crossing of the pairs, which would help with the katabatic prevailing wind alignment issues...
This is also a very interesting possibility. We have deliberately chosen not to work with cross-track measurements, because we assume that the obstacles that contribute to form drag are much narrower than the pair spacing (90 m), hence undetectable in cross-track direction. Nevertheless at cross over points, the smaller scale obstacles could be retrieved in cross directions. The methods described in this manuscript would however need to be completely revised in order to estimate z_0, as this would not result in typical 200 m profiles. Undoubtedly a method could be developed to extract 3D roughness information at cross-over points, we believe this is outside the scope of this study.

L382:
The algorithm described in Sect. 3 could be adapted to extract these features from the ATL03 data. For instance, smaller-scale obstacles could be retrieved in multiple directions at cross-over points, using the information from multiple

ICESat-2 tracks. However, this is beyond the scope of this study, which is to map the aerodynamic roughness of rough ice over large scales.

The primary roughness retrieval algorithm (i.e., thresholding photons according to confidence class, median filtering, then interpolating with k-nearest neighbor and kriging in constructing profile obstacles) seems reasonably considered, and robust. The alternative formulation which uses the standard deviation of photon spread from the de-trended ATL03 product is less compelling; there is no accounting that I can tell for difference in signal strength or atmospheric conditions; photons for the standard deviation calculation are weighted equally regardless of the per photon quality/confidence flags. While this residual measure is designed primarily to provide an upper bound of the estimated surface roughness, rather than a 'best estimate' of surface roughness, additional corrections and filtering of what photons to consider would improve the metric.
We agree for the most part with the reviewer, yet weighting individual photons does not improve the metric using our methods. We have experimented with a weighted standard deviation in our Eq. (8). Using weights of $q\_flag/4$, where q_flag is the confidence level, does not lead to a convincing improvement. The reason is that due to our photon selection strategy (Lines 209-212), we are rarely using photons from different noise levels in each 200 m profile. This can be seen in Fig 7a2, and in our new Fig. B2, as in area B only *high confidence* photons are used in the calculation.

Around lines 375 to 380 there is a discussion of how the ATL03 surface roughness retrieval breaks down at higher elevations...however it is unclear if this is due to sensor tuning for the specific algorithm, or theoretical limits for conceptual mental model that relies on obstacle formalize instead of skin friction parameterization. High resolution DEMs at the higher elevation bands would likely indicate if the formalism adopted in section 2.2 can be scaled to sastrugi in principle, or if the conceptual framework itself is no longer appropriate given the dominance of skin friction related to inherent snow and firn properties. In other words, lack of high elevation UAV DEM coverage such as exisits at the lower S5 or sites 'A' and 'B' does not allow the reader to infer if the Bulk Drag Partitioning method itself is not suited to retrievals at these heights, or if algorithmic implementation as presently tuned is not suited. (Note, this is issue is also raised by the other two referees). Determining this does not require coincident data; simulation of the method on a generic surface with ice hummocks at 0.6m scale would provide enough context to discuss the issue in the text.
This is an interesting modelling exercise, unfortunately the exact shape and size of the obstacles at sites higher than SHR remains unknown, due to the lack of UAV surveys at higher locations. As such the mentioned obstacle height of 0.6 m at S6 is a very crude estimate based on fieldwork photographs, and also known to considerably change after large melting events or snowfall.
Nevertheless, we believe a first order guess can still be beneficial, therefore we

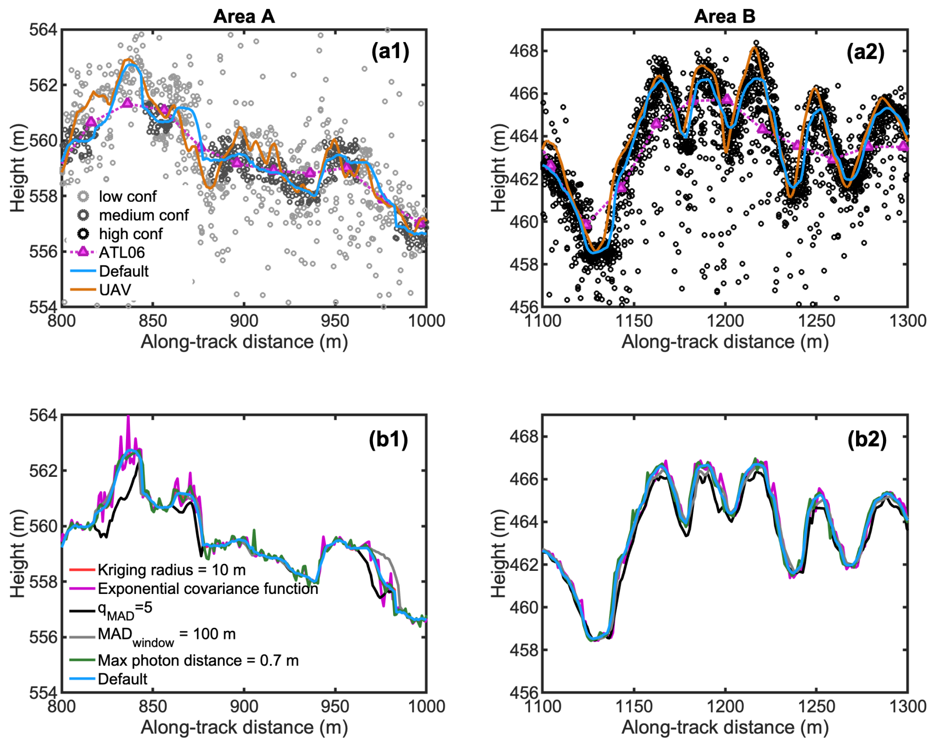

Figure B2: Elevation profiles in a 200-m portion of area A (left) and area B (right). The top panels contain the ATL03 data sorted in confidence levels (dots), the ATL06 data (pink triangles), the profiles measured by UAV photogrammetry (orange line) and the 1-m interpolated ATL03 data using the default settings used in the main text (blue line). The bottom panels contain the 1-m interpolated AT03 data using different origins and photon filtering settings.

propose to add a figure and a few sentences in the Appendix A, just after the description of the bulk drag model. We also propose to refer to this figure in Section 4.4.

L475:
Following the steps above, z_{0m} can be estimated for any H and λ, which is done in Fig. A1. At areas A, B and site S5, H and λ are estimated from the UAV surveys and from ICESat-2 data. At site S6, we assume that $H = 0.6 \pm 0.1$ m and $\lambda = 0.045 \pm 0.015$, based on photographs taken during the end of the ablation season. At the highest site S10, we assume that $H = 0.3 \pm 0.2$ m and $\lambda = 0.02 \pm 0.01$, which are typical values for sastrugi (Andreas, 1995).
L378:
Higher up, the ice hummocks become even smaller and the surface eventually becomes snow-covered year-round. Nevertheless, snow sastrugi, known to reach

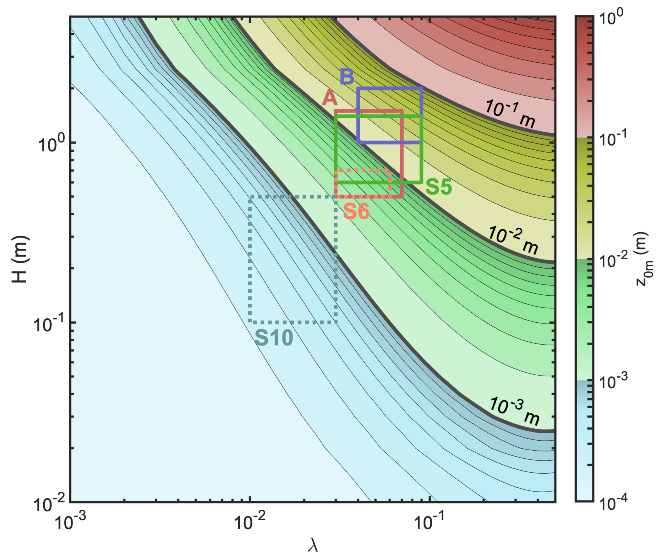

Figure A1: Estimated z_{0m} using the R92 model with parameterized C_d (Appendix A), as function of obstacle height H and frontal area index λ.The solid squares denote the estimated H and λ at three sites using UAV surveys. The dashed squares are first-order guesses based on photographs. See Fig. 1 for the location of each site.

up to 0.5 m height at site S10 from photographic evidence, still contribute to form drag. This results in a maximum observed value of $z_{0m} = 7 \times 10^{-4}$ m at sites S9 and S10 (Fig. 10). Using a rough estimate for both H and λ at S6 and S10, based on photographs taken during the end of the ablation season, yields more realistic values for z_{0m} (Fig. A1) than using H and λ from the ICESat-2 elevation profiles. Therefore we conclude that the roughness obstacles are not properly resolved at these locations in the ATL03 data using the algorithm presented in this study, even when the correction using the residual photons scatter is applied.

Technical Corrections:

Line 1: Curious if the authors mean 'latent heat' explicitly when they reference moisture in this context

Yes, we refer here to the roughness length that is required to estimate the surface latent heat flux from vertical gradients of specific humidity.

Line 25: 'form drag' is more formally defined later in equation 3; I would include the parameter name (tau_r) here as well to aid readers.
Added
Due to the effect of form drag (or pressure drag) τ_r, ...

Line 35: This is vague– are there no physically based drag models that are capable of simulating surface roughness length from an elevation profile period? Or just no models that are used for simulating the exchange between cryospheric surfaces and the atmosphere?
We propose to remove this sentence in order to avoid any confusion.

L35:
~~Unfortunately, to-date there is no physically based drag model used for atmospheric models over glaciers and ice sheet. Instead,~~ Over glaciers, semi-empirical approaches based on Lettau (1969) are often used, such as by Munro (1989), Fitzpatrick et al. (2018) and Chambers et al. (2019).

Figure 1: The 'large black box' referenced isn't clear, and is easily mistaken as a graticule; use a different bright color (orange, yellow, red) with higher saturation to highlight the area better.
We agree with the reviewer and have adapted the figure accordingly.

Line 95: While the fetch footprint is variable, discussion of the range or a small table of the normal values as a function of boundary-layer height / friction velocity would be helpful.
The shape of the fetch footprint depends on many parameters, and we refer to the paper (and code) from Kljun et al., 2015 for the exact equations. We propose to add the extent of the fetch footprint that contributes to 80% of the flux in a very specific wind direction in Fig. 2. We refer to this additional information in L93 and L133 of the revised manuscript.

L93:
This geometry is a strong simplification of the true fetch footprint, which is calculated for a specific wind direction at S5 in Fig. 2, after Kljun et al. (2015). This simplification allows us to use 1D elevation datasets, such as profiles from the ICESat-2 satellite laser altimeter. Besides, the true fetch footprint depends on flow parameters such as the friction velocity (u_*) and the boundary-layer height (Kljun et al., 2015), which are not known a priori.

L133:
(...) where w is the width of the profile, set to 15 m. This value was chosen to match the approximate ICESat-2 footprint diameter, yet it is much smaller than width of the real fetch footprint (Fig. 2).

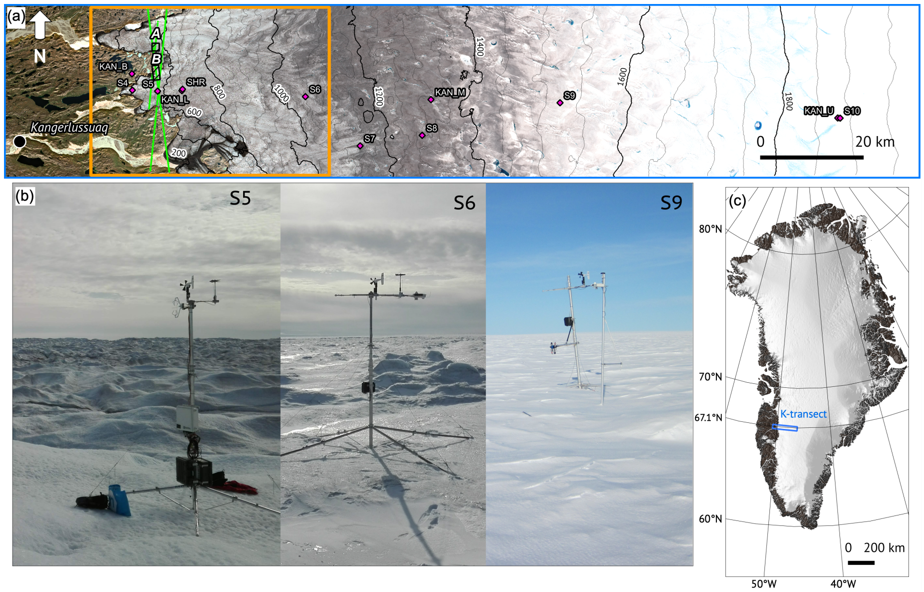

Figure 1: (a) Map of the K-transect, with the location of the automatic weather stations and mass balance sites indicated by the pink diamonds. The black boxes A and B delineate the areas mapped by UAV photogrammetry. The large black box indicates the area covered in Figs. 5 and 9. The background image was taken by the MSI instrument (ESA, Sentinel-2) on 12-08-2019. Pixel intensity is manually adjusted over the ice sheet for increased contrast. The green solid lines denote the ICESat-2 laser tracks that are compared to the UAV surveys (Table 2). (b) Sites S5 (06 Sep 2019), S6 (06 Sep 2019) and S9 (03 Sep 2019) taken during the yearly maintenance. Note that no data from the the AWS shown at S9 is used in this study. (c) Location of the K-transect on the Greenland ice sheet.

Figure 3: Standard convention is that 'noise' photons are labeled as grey, and 'signal' photons are labeled as black. I realize that color choice here is carried forward with consistency for the figures that follow, so that yellow and grey lines reference the same process/data in figures 4, 7, and 8, but I think that these figures need to have the colors switched as well. The data/noise convention for photon signal/noise is similar in strength to mapping conventions that expect water labeled as blue, or data orientation to point North. If there are concerns for black data dots being too dark in Figure 4 and obscuring the profile, using blue data points is a possible work around (dark blue for signal, cyan or light blue for noise)...but in general, convention and expectation is that the lighter saturation or value assigned in point plots is for noise, and darker points are signal.

We agree with the reviewer and have changed the colors in figures 3, 4. However in figures 7 and 8 we do not discern signal from noise.,, and adding more colors

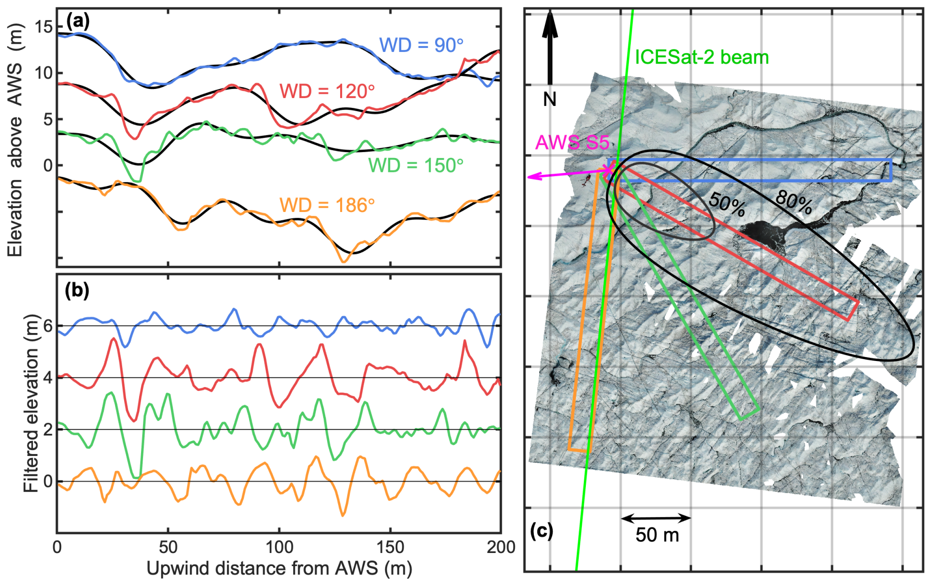

Figure 2: (a) Measured elevation profiles for four different wind directions upwind of AWS S5, (b) Filtered elevation profiles and (c) orthomosaic true-color image of AWS S5 and surroundings taken by UAV photogrammetry on 6 September 2019. The different coloured rectangles in (c) indicate the profiles shown in panel (a). The profiles have been vertically offset by 5 m in (a) and by 2 m in (b) for clarity. The black line in (a) denotes the low-frequency contribution of the profiles for a cut-off wavelength $\Lambda = 35$ m. The pink arrow in (c) denotes the displacement vector of the AWS between the ICESat-2 overpass on 14 March 2019 and the UAV imagery on 6 September 2019. The estimated extent of the 50% and 80% fetch footprints for the data in Sep 2019 in wind directions $\in [179; 181]°$ is shown by the black ovals.

would make these figure difficult to interpret. So we propose to keep the same style for figures 7 and 8.

Line 120: Can the cut off wavelength be variable? This question is probably related to my comment on lines 375-380 that I discussed at the end of 'specific comments'

There is no definite theory on which value for Λ should be used, therefore this is a tuning parameter in our model. After the comment of Referee # 1, we have added a sensitivity analysis in a new Appendix B that explores the output of the bulk drag model for different values of Λ (see our new Fig. B1)

Line 145: "...140 km transect AWS..." –¿ "...140 km transect of AWS..."

Changed

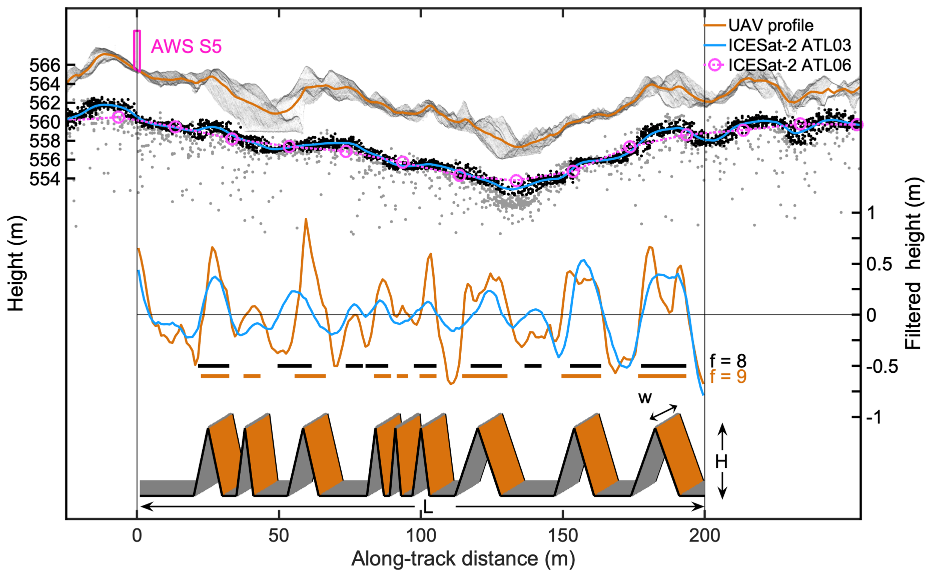

Figure 3: Steps in converting a measured digital elevation model to the modelled topography, where L is the length of the profile, f the number of obstacles, H the height of the obstacles and w the width of the elevation profile. The location and height of AWS S5 is shown on top of the UAV elevation profile. The black dots denotes all the ATL03 photons, while the grey dots denote the selected photons for the kriging procedure. The solid black line denotes the 1 m resolution interpolated profile for ATL03 data, and the pink dots denote the 20 m resolution ATL06 signal.

Line 200: Some discussion/mention of wet surfaces and standing water is warranted here
Added. See also reply to the 2nd comment in "Specific Comments" above

Line 225: This should modified to account for signal strength; since the ratio of noise to surface photons varies with signal strength, the standard deviation will be biased between high and low signal strength acquisitions over the same surface. This is true for the background count rate as well, which varies seasonally and between night and day conditions.
see our reply above concerning the weighting of signal photons.

Line 240: I'm unclear on exactly what is meant be residual photons here, and if they are weighted or binned by the confidence flags assigned in ATL03.

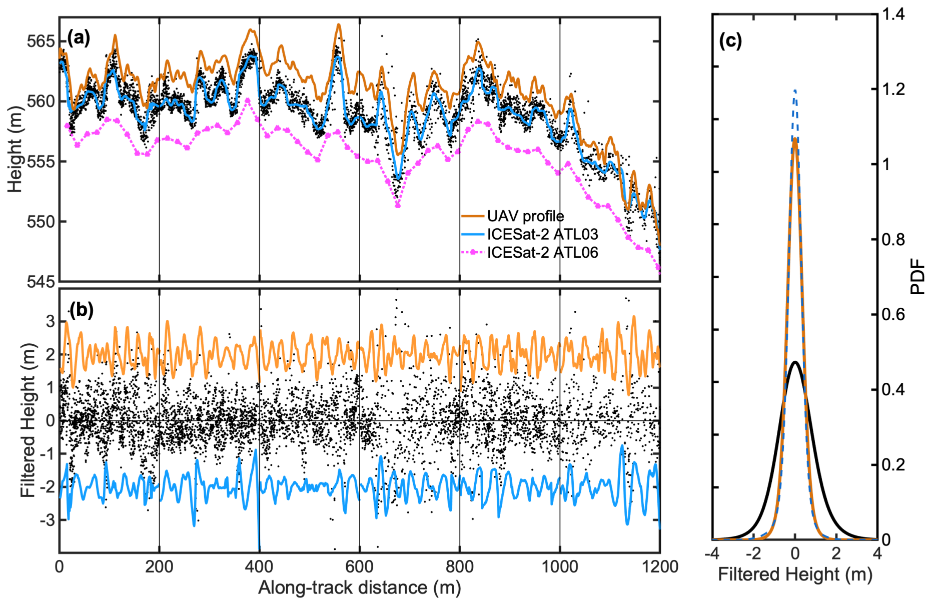

Figure 4: (a) Elevation profile at site A measured by the UAV and by ICESat-2 (solid lines), selected ICESat-2 photons (grey dots) and ICESat-2 ATL06 height (pink dashed line). The UAV and ATL06 profiles have been vertically offset by 2 m for clarity. (b) Filtered profiles (solid lines) and residual photons elevations after filtering per 200 m windows (grey dots), where the UAV and ATL03 filtered profiles have also been vertically offset. (c) Probability density function of the filtered ICEsat-2 profile (black dashed line), UAV profile (orange solid line) and residual photons elevations (grey line).

Here we refer to the residual photon elevations, that we defined as the signal of the selected photons minus the interpolated 1 m resolution profile. We propose to refer to this definition in L240.

L240:
On the other hand, the residual photon elevations, defined as the selected photons detrended for the interpolated profile under Eq. (8) still contain much larger scatter than the UAV elevation profile. This demonstrates that roughness is not the only factor explaining the scatter in the raw altimeter signal.

Line 255: First use of 'L69' I think...a sentence somewhere defining the acronym convention for the various methods would help
The first reference to Lettau (1969) can be found in Line 89.

Line 270-275: I don't know if it's true to say that there's no relationship between

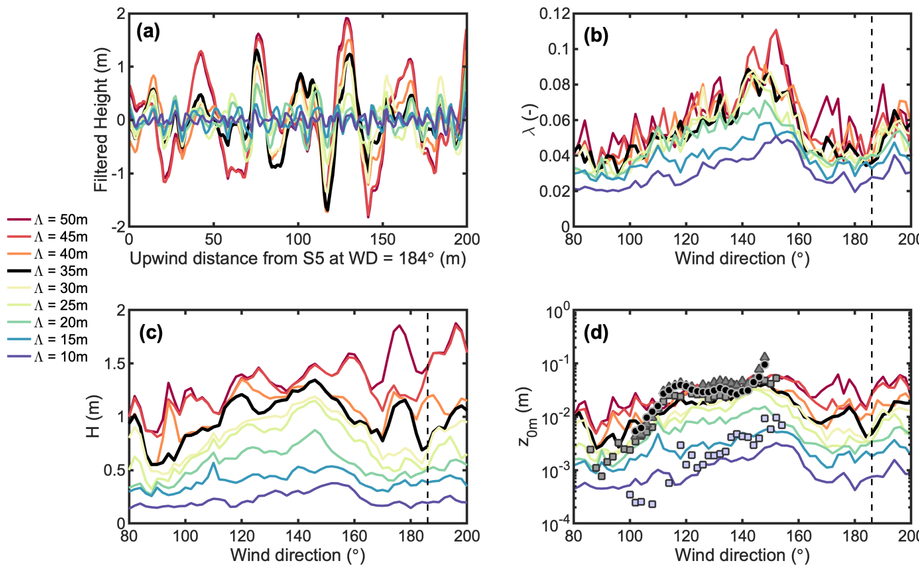

Figure B1: (a) Filtered elevation profile in fetch direction 186°, (b) estimated obstacle frontal aera index, (c) estimated obstacle height and (d) modelled aerodynamic roughness length at site S5 for different high-pass cutoff wavelengths Λ. See Figure 8 in main text for the labels in d).

C_d and either H or lambda...especially when the next sentence links increased C_d values with increases in H. I'd change this to say that the there is a weak relationship.
We agree with the reviewer and have modified this sentence.

L271:
In Sect. 4.3 we estimate the values for C_d required to fit the model to the observations; these values vary between 0.1 and 0.3, and show a weak relationship with H.
Line 288: I think figure 5 is meant here, not figure 6
The reviewer is correct. We have corrected this.

L288:
The elevation profile from the UAV survey in box A (Fig. 5) was already compared to the overlapping ICESat-2 profiles in Fig. 4a, while H, λ and z_{0m} are compared in Fig. 7.

Line 313: Eddy covariance measurements are available outside of September, I assume? Even if they aren't available in March specifically, having a date range of the measurement record would be helpful, instead of just the date that the data was pulled for this study.

At this time we have (recent) sonic eddy covariance (SEC) data during September-October 2019 at sites S5 and SHR, and we have year-round flux measurements using the vertical propeller eddy covariance method (VPEC) at sites S5 and S6 since September 2016. We have added this information in the revised manuscript.

L143:

Vertical propeller eddy covariance (VPEC, see also T20) measurements are available at sites S5 (67.094° N, 50.069° W, 560 m) and S6 (67.079° N, 49.407° W, 1010 m) since 2016, while AWS observations are available since 1993 and 1995 for each site (Smeets et al, 2018). For this study we use eddy-covariance measurements acquired during September 2019 at site S5 and also site SHR (67.097° N, 49.957° W, 710 m), and during from September 2018 to August 2019 at site S6. All these sites are situated in the lower ablation area of the K-transect, (...).

Figure 8: This would be appropriate to split into a.) and b.) panels. I'm skeptical of the pink 'perfect fit' line; the eddy covariance measurements that the C_d values are inferred from have some spread or standard deviation, so I expect that modeling those uncertainties would produce a flatter line or a bounding envelope.

We agree with the reviewer, and we have modified Fig. 8 in order to present the optimal values for C_d using all three in situ datasets.

Line 385: This claim should be tempered a bit. Sure, there is lower contribution to runoff at higher elevations, but the increased surface area relative to the margin means that modeling the high elevation roughness is crucial for understanding and modeling the overall energy exchange between the cryosphere and atmosphere. Also, under changing climate scenarios, run off contribution will increase for high elevations.

We agree with the reviewer and therefore propose to remove this sentence.

L386:

~~Besides, these high-elevations areas contribute much less to the total melt and runoff, due to the brighter surface and lower temperatures.~~

Line 430: Capitalization is inconsistent between equation A1 and the following line where the parameters are defined.

Revised.

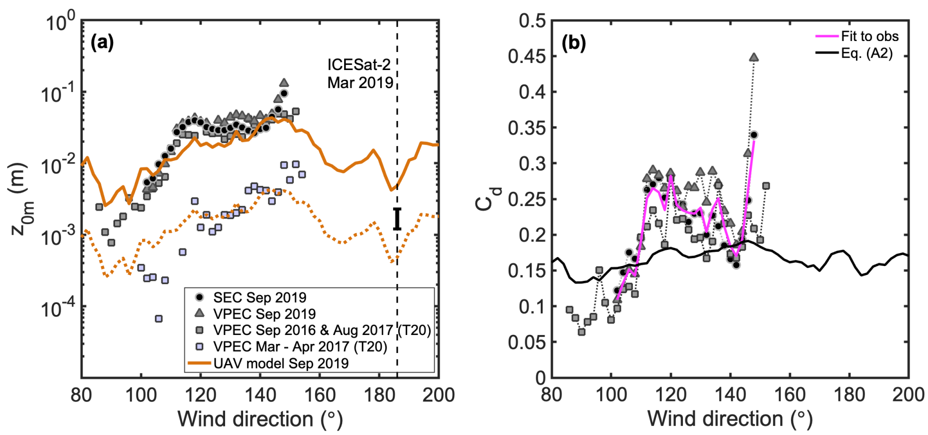

Figure 8: (a) Drag model evaluation at site S5. (b): Drag coefficient for form drag (C_d) used in the model (black line) or required to perfectly fit the observations. The orange solid line is the modelled z_{0m} using the R92 model and UAV photogrammetry on 06 September 2019, while the dashed orange line is the orange line shifted down by a factor 10. Solid symbols are measurements from sonic eddy-covariance (SEC) or vertical propeller eddy-covariance (VPEC). Additional data is from Van Tiggelen et al. (2020, T20). The vertical dashed line denotes the direction sampled by the ICESat-2 laser beam on 14 March 2019. The errorbar denotes the range between the uncorrected and corrected ICESat-2 measurements.